


AUTHOR QUERY FORM

	Journal: WEA Article Number: 100694	Please e-mail or fax your responses and any corrections to: E-mail: corrections.esch@elsevier.macipd.com Fax: +44 1392 285878
---	--	--

Dear Author,

Please check your proof carefully and mark all corrections at the appropriate place in the proof (e.g., by using on-screen annotation in the PDF file) or compile them in a separate list. Note: if you opt to annotate the file with software other than Adobe Reader then please also highlight the appropriate place in the PDF file. To ensure fast publication of your paper please return your corrections within 48 hours.

For correction or revision of any artwork, please consult <http://www.elsevier.com/artworkinstructions>.

Any queries or remarks that have arisen during the processing of your manuscript are listed below and highlighted by flags in the proof. Click on the [Q](#) link to go to the location in the proof.

Location in article	Query / Remark: click on the Q link to go Please insert your reply or correction at the corresponding line in the proof
Q1	Please confirm that given names and surnames have been identified correctly and are presented in the desired order.
Q2	Fig. [6] has been submitted as color image; however, the caption has been reworded to ensure that it is meaningful when your article is reproduced both in color and in black and white. Please check and correct if necessary.

Thank you for your assistance.

Please check this box or indicate your approval if you have no corrections to make to the PDF file



ELSEVIER

Contents lists available at SciVerse ScienceDirect

Wear

journal homepage: www.elsevier.com/locate/wear

Highlights

Effect of relative humidity and applied loads on the tribological behaviour of a steel/Cr₂O₃-ceramic coupling

Wear ■ (■■■■) ■■■–■■■

Mattia Merlin, Chiara Soffritti, Reyna Vazquez

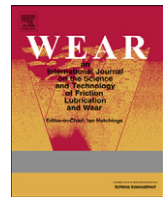
Department of Engineering, University of Ferrara, Via Saragat 1, I-44122 Ferrara, Italy

- Tribological behaviour of a steel in contact with a plasma-sprayed Cr₂O₃ coating.
- Different conditions of applied normal load and relative humidity.
- In dry conditions, the metallic film transfer onto ceramic surface is observed.
- In wet conditions, metal transfer is depending on the normal load applied.
- Ceramic coating undergoes microfracture along splat and columnar grains boundaries.



Contents lists available at SciVerse ScienceDirect

Wear

journal homepage: www.elsevier.com/locate/wear

Effect of relative humidity and applied loads on the tribological behaviour of a steel/Cr₂O₃-ceramic coupling

Q1 Mattia Merlin*, Chiara Soffritti, Reyna Vazquez

Department of Engineering, University of Ferrara, Via Saragat 1, I-44122 Ferrara, Italy

ARTICLE INFO

Article history:

Received 24 July 2012

Received in revised form

14 March 2013

Accepted 25 March 2013

Keywords:

Diesel engine

Steel

Plasma-spray coating

Friction

Wear

Metal transfer

ABSTRACT

The friction and wear behaviour of a carbon steel in sliding contact with a plasma-sprayed ceramic coating (Cr₂O₃) is investigated under different conditions of normal load and relative humidity, through a pin-on-disk equipment. The samples are analysed by means of Optical Emission Spectroscopy (OES), Optical Microscope (OM), Scanning Electron Microscope (SEM) with Energy Dispersive Spectroscopy (EDS), X-ray Diffraction (XRD), surface roughness, fracture toughness and microhardness tester. The friction was continuously monitored during the tests while the wear rate of the coatings was evaluated by measuring the wear scar profiles after the tests. The wear rate of the pins was determined by weighing them before and after the wear tests. For all the normal loads applied in dry conditions, the metallic film transfer onto the ceramic surface was observed. In wet conditions, the metal transfer largely depended on the normal load applied. Microcracks were noticed along the splat and columnar grains boundaries on the Cr₂O₃ wear scars. The observations of the worn surfaces of the pins indicate a mild-oxidational wear mechanism with the appearance of ploughing and plastic deformation.

© 2013 Published by Elsevier B.V.

1. Introduction

Over the last decade much effort has been made to improve the performance of diesel engines in terms of fuel efficiency and low emissions. This includes the possibility to operate on engine subsystems such as the engine block with its pistons and cylinders, the transmission, the fuel system, the valve train and the exhaust system. Many studies have focused on the use of multi-component alloys in valves and valve seats [1–3]. Such alloys are resistant to high temperatures and the corrosive environment of combustion gases but are very expensive. For example, several authors have investigated the effect of high-temperature oxidation on the sliding wear of superalloys [4–6]. They have dealt with the ability of so-called ‘glaze’ layers to protect the surfaces during sliding wear at high temperatures and under relatively low loads and sliding speeds.

It is well known that heat, either frictional or externally applied, has a great influence on the wear processes of metallic components. High temperatures can facilitate oxidation of the contacting surface, causing a considerable decrease in the wear rate and giving a transition from severe to mild wear. This change is usually associated with the generation of oxide and

partially-oxidized metal debris on the coupling surfaces. At higher temperatures a glaze, a top layer of compacted particles, can form on the surface reducing friction and wear rates. However, when the sliding speed at room temperature is very high, the oxide glaze can begin to come off, leading to severe-oxidational wear [7–10]. The ability of this oxide to act as a barrier and protect against wear is due to the rate of diffusion of the reactants across the barrier layer. Iron and mild steel form protective glazes (tribo-layers) of Fe₃O₄ on exposure to air at temperatures above 500 °C. These are effective barriers to diffusion, but the phase FeO becomes stable at higher temperatures. It develops at the metal/Fe₃O₄ scale interface and is a poor barrier to diffusion of reactants [11,12].

The effects of oxygen in reducing the wear of metallic components have been investigated for many years. However, in practical applications humidity also has a great effect on the wear rates of metals. Some authors have proposed that increasing humidity inhibits the delamination and adhesion wear of steels. They have suggested that it is due to the reduction of the oxidation rate on the steel worn surface and to the formation of iron hydroxide and ferri-oxide-hydrate. These oxides and water adsorption act as protective layers that prevent the metal/metal interaction [13,14]. Goto and Buckley [15] found the opposite, which is a direct correlation between wear and humidity: the lack of oxygen adsorption in the presence of water vapour can reduce the rate of oxidation and thus increase the wear. On the other hand, Bregliozzi et al. [16] found that both the wear and friction coefficient for un-lubricated sliding of stainless steel significantly

* Corresponding author. Tel.: +39 0532 974831; fax: +39 0532 974870.

E-mail addresses: mattia.merlin@unife.it (M. Merlin),

chiara.soffritti@unife.it (C. Soffritti), vzqmr@unife.it (R. Vazquez).

dropped, though the oxidation rate reduces with increasing humidity. Finally, other authors have demonstrated that the sliding speed significantly influences the effect of humidity in the sliding wear of steels: at a high sliding speed, the wear increases with humidity, while the opposite is observed at a low sliding speed [17].

An interesting alternative to the use of ferrous alloys or super-alloys in engine subsystems is the employment of ceramic coatings that are thermally sprayed on cheaper and shock resistant materials, such as carbon steels. Some ceramics have already found engineering applications as tribological components, such as cutting tool inserts, rolling bearings, braking devices, water pumps, ash scrapers, cylinder head fire decks, piston crowns, exhaust valve faces and so on [18]. Moreover, thermal-sprayed coatings are resistant to many corrosive environments, they have chemical stability and very high hardness and can stand high temperatures. However, it is difficult to choose a suitable coating. In literature many studies have investigated the friction of hard materials, such as ceramics against steels [19–23]. There have been examinations of the existence of many cracks at the metal surface or the formation of grooves and wear debris with subsequent metal removal. The metal particles were transferred onto the ceramic by adhesion. Only scratches due to plastic deformation were seen on the ceramic surface. It was also shown that the transfer between metal and ceramic depended on the load (more precisely on the Hertzian pressure) and on the temperature at the interface. It also depended on the specific properties of the ceramic, like its hardness, roughness, affinity with the metal, the cohesion among the grains and the tensile strength of the antagonist. Fernandez et al. evaluated the wear behaviour of plasma-sprayed Cr_2O_3 coatings against steel in a wide range of loads and sliding speeds. The results demonstrated that the wear of the coatings increased with an increasing load. Moreover, in dry sliding of the Cr_2O_3 coating there was a minimum-wear sliding speed (about 0.5 m/s) and a maximum-wear sliding speed (about 3 m/s) [24].

The aim of this work is to evaluate the tribological behaviour of the plasma-sprayed Cr_2O_3 coating against a carbon steel under different sliding wear conditions, through pin-on-disk testing. Compared to the loads that occur in diesel engine applications, relatively low normal loads are used due to the limitations of the

test equipment. However, this can provide useful indications of the potential of the coating in sliding wear applications. All tests are carried out at room temperature and at 15% and 95% relative humidity. The effect of both the environmental conditions and the applied load on the wear mechanisms is discussed.

2. Materials and experimental details

A plasma-sprayed Cr_2O_3 ceramic coating with a thickness of 150 μm (powder: Amperit[®], $-45+22.5$ μm , fused and crushed) on a Ni-20%Cr bond coat about 20 μm -thick (powder: Metco 43CNS, $-106+45$ μm) to improve the ceramic material adhesion, are deposited onto circular steel plates (80 mm in diameter and 6 mm in thickness). The spray parameters are confidential. The chemical composition of the steel plates was determined by Optical Emission Spectroscopy (OES), whereas the composition of the feedstock powder was directly provided by the manufacturer. Details of the steel plates and feedstock powders chemical composition are reported in Table 1.

The coating microstructure was investigated by a Philips X'PERT PW3050 diffractometer, using Cu K α radiation ($\lambda=1.54$ Å), with an intensity scanner vs diffraction angle between 15° and 120° (step size of 0.06°, scanner velocity of 2 s/step and 1.5 grid), a voltage of 40 kV and a 30 mA filament current. The LEICA MEF4M Optical Microscope was also used on properly polished cross-sections. The micrographs were elaborated by means of Image-Pro Plus v6.0 image analysis software to evaluate coating porosity. Roughness parameters (R_a and R_z) were calculated by the portable Handysurf E35_A ZEISS-TSK rugosimeter. Before each measurement all the coating surfaces were cleaned in an ultrasonic bath. Microhardness (3 N load and 15 s loading time) and fracture toughness (10 N load) measurements were performed on polished cross-sections of the coating by means of a Future-Tech FM-model Vickers microindenter. A mean of 15 indentations were carried out for each microhardness and toughness measurement. In particular, fracture toughness was evaluated by measuring the indentation diagonals and the length of the crack from optical micrographs, employing the Evans–Wilshaw equation:

$$K_{IC} = 0.079(P/a^{3/2})\log(4.5a/c) \quad (1)$$

Table 1
Steels and feedstock powders used to produce top and bond coatings.

	Composition
Cr_2O_3	0.06% SiO_2 ; 0.03% Fe_2O_3 ; < 0.02% TiO_2 ; balance Cr_2O_3
Ni-20%Cr	19.07% Cr; 1.1% Si; 0.4% Fe; 0.02% C; balance Ni
Disk	0.22% C; 0.88% Mn; 0.87% Ni; 0.84% Cr; 0.30% Si; 0.20% Cu; 0.06% Mo; 0.03% S; 0.02% V; 0.02% P; balance Fe
Pin	0.23% C; 0.86% Mn; 0.95% Ni; 0.91% Cr; 0.26% Si; 0.10% Cu; 0.06% Mo; 0.02% S; 0.02% V; 0.01% P; balance Fe

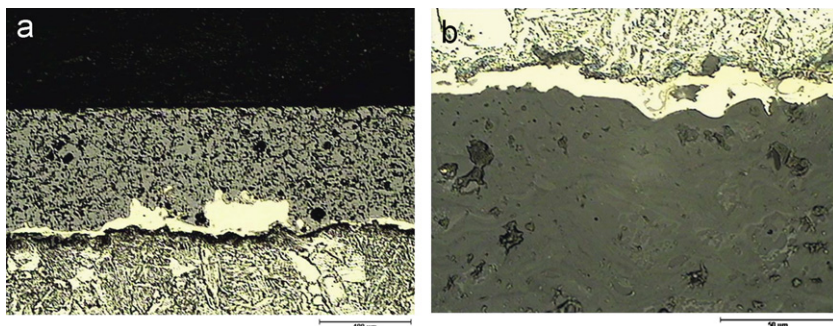


Fig. 1. Optical micrographs showing cross-sections of Cr_2O_3 coating and Ni-20%Cr bond coat.

where a is the half diagonal of the indentation (μm), c is the crack length (μm) and P is the load (mN). This formula is developed for “half-penny-shaped” cracks, but it is reported in literature that this is also valid for Palmqvist cracks. The unique limitation is that the ratio between the crack and the half diagonal length must be between 0.6 and 4.5 [25,26].

Pin-on-disk dry sliding tests were performed with a Multi-specimen Tester tribometer produced by DUCOM Instruments, in accordance with ASTM G99-05 “Standard test method for wear testing with a pin-on-disk apparatus”, using cylindrical steel pins of 6 mm in diameter and 22 mm in height as a counterpart material. The chemical composition of the pin is listed in Table 1. All the pin surfaces were cemented for about 500 μm in thickness. The Vickers microhardness of the pins was determined (1 N load and 15 s loading time) on cleaned cross-sections, at a distance of 100 μm from the coupling surface. Four different sets of tribological parameters were used, varying the normal load and relative humidity (RH). In particular, normal loads were fixed at 450 N and 650 N, corresponding to the initial Hertzian pressure of 3.98 MPa and 5.75 MPa at the center of the pins, respectively. The values of 15% and 95% relative humidity were also selected. For each test, the sliding speed of 1 m/s and the sliding distance of 7500 m were kept constant. All tests were carried out at room temperature. The equipment directly calculated the friction coefficient. The wear rate of the pins was evaluated by weighing the specimens before and after the tests. Weight loss was converted into volume loss by dividing it by the density of the material. The wear rate of the disks was evaluated by measuring the area of the wear track cross-section with a Hommelwerk T2000 profilometer. Each area, obtained as an average value of four measurements along the wear circumference, was used to calculate the wear volume. In order to understand the main wear mechanisms, the worn surfaces of the coating were investigated by means of X-ray Diffraction (XRD). The wear tracks on the pin and coating surfaces were also observed by a Scanning Electron Microscope (SEM) equipped with an Energy Dispersive Spectroscopy (EDS) microprobe. Finally, the worn cross-sections of the pin were characterised by OM analyses and Vickers microhardness measurements.

3. Results and discussion

3.1. Microstructure and mechanical properties

Fig. 1a and b shows the two optical micrographs of the investigated Cr_2O_3 coating showing the typical lamellar microstructures of a plasma-sprayed ceramic coating. It is characterised by a homogeneous microstructure with a prevalence of inter-lamellar cracks and uniformly distributed pores. Inter-lamellar cracks, caused by thermal residual stresses, are the main reason for the low intersplat cohesion of the coating. The Ni-20%Cr bond coat is markedly irregular in order to facilitate the adhesion of the

coating to the substrate (Fig. 1a). At higher magnification the optical micrograph of the steel/bond coat interface shows evidence of pores and sandblast residues (Fig. 1b). The coating porosity determined by image analysis is about 11%, due to splat stacking faults and gas entrapment [27]. The XRD analysis of the coating surface, depicted in Fig. 2, reveals that it is fully consisted in the eskolaite phase (Cr_2O_3). Hardness, roughness parameters and fracture toughness of the coating are listed in Table 2. After the Vickers indentations for the measurement of fracture toughness, micrographs of the coating cross-sections showed that cracks preferentially propagate along the splat boundaries, parallel to the substrate interface. This is further evidence of the low intersplat cohesion.

Micrographs collected in Fig. 3a and b describe the microstructure of a steel pin near the coupling surface. Fig. 3a allows evaluation of the thickness of the hardened layer of about 500 μm . At higher magnification the cemented layer exhibits a martensitic microstructure with a small amount of carbides (Fig. 3b), whereas the unaffected material has a homogeneous lower bainitic microstructure. Table 2 shows Vickers microhardness of the martensitic +carbide microstructure, near the coupling surface.

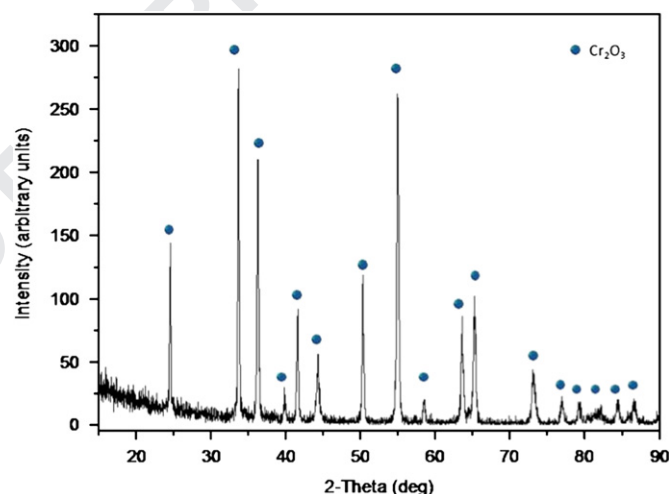


Fig. 2. XRD pattern of Cr_2O_3 coating.

Table 2

Mechanical properties and roughness of ceramic coating and steel pins.

	HV _{1N} [GPa]	HV _{3N} [GPa]	R _a [μm]	R _z [μm]	K _{IC} [MPa m ^{1/2}]
Cr_2O_3	—	11.88 ± 0.45	0.15 ± 0.02	1.78 ± 0.19	7.16 ± 0.88
Pins ^a	6.70 ± 0.05	—	—	—	—

^a Vickers microhardness is evaluated on cross-section of pin, at a distance of 100 μm from the coupling surface.

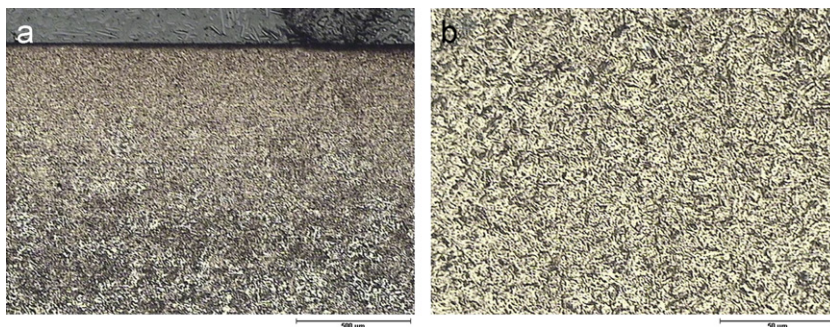


Fig. 3. Optical micrographs showing cross-section of steel pins in cemented zone: (a) 50 \times , (b) 500 \times .

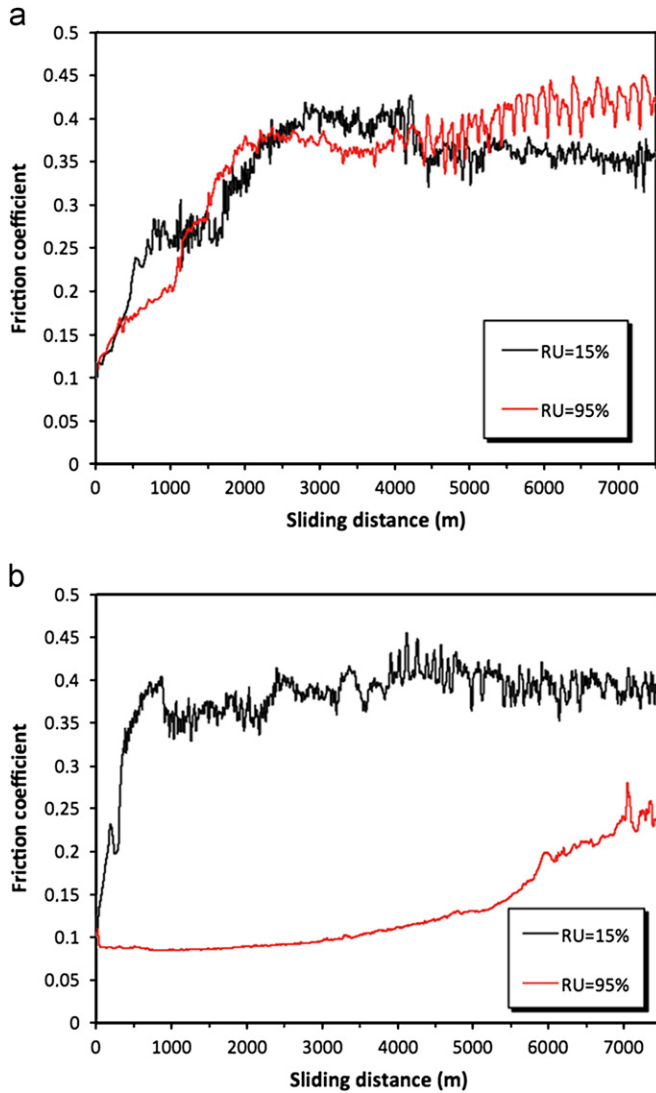


Fig. 4. Friction coefficient variation in different conditions for (a) 650 N and (b) 450 N normal loads.

3.2. Pin-on-disk wear tests

Fig. 4a and b depicts the friction coefficient calculated by the equipment during the tests. When a 650 N normal load is applied in dry and wet conditions (Fig. 4a), the friction coefficient considerably fluctuates around the average value. These fluctuations are associated with high frequency squeaky noise developed concurrently with the rise of the friction coefficient and the metallic film deposition on the ceramic surfaces. Both curves follow the same pattern. At the beginning of each test the friction coefficients are quite low ($\mu \cong 0.1/0.2$) and then progressively increase as the test proceeds. After about 2000 m, the values reach a quasi steady-state ($\mu \cong 0.3/0.4$). These values remain constant until the end of the tests. When a 450 N normal load is applied in dry conditions (Fig. 4b) the friction coefficient rises rapidly during the first few minutes and reaches the quasi-steady-state at only 500 m. When a 450 N normal load is applied in wet conditions the tribological behaviour is very different. The friction coefficient remains constant at a very low value ($\mu \cong 0.1$) until the sliding distance of 3000 m. It then rises slowly until reaching the value of about $\mu \cong 0.2$ at the end of the test.

Fig. 5a shows the total wear when a 650 N normal load is applied, in dry and wet conditions. Also in this case, both curves

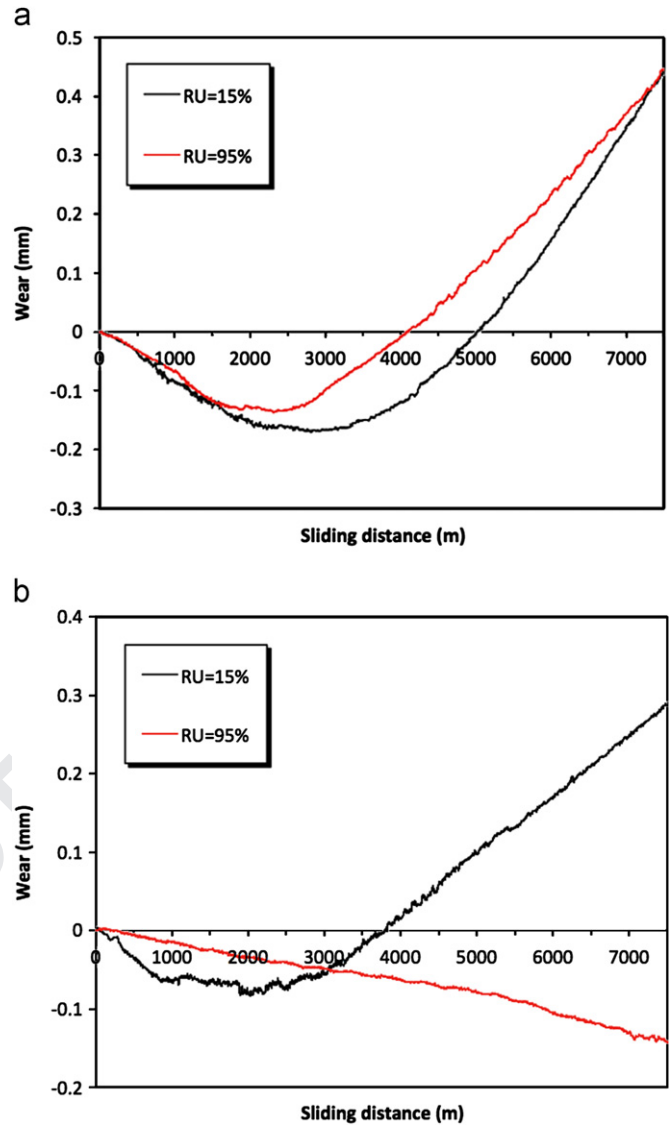


Fig. 5. The amount of wear in different conditions for (a) 650 N and (b) 450 N normal loads.

follow the same pattern. Wear is negative up to a sliding distance of about 3500 m in dry conditions, then it progressively increases as the test proceeds. At the end of the tests wear is positive and equal to 0.45 mm. In wet conditions wear reverses its trend for a sliding distance of about 2500 m and at the end of the test it reaches approximately the same value as the previous case. When a 450 N normal load is applied in dry conditions (Fig. 5b) the wear rises rapidly after about 2500 m up to the positive value of 0.29 mm. As for the friction coefficient, when a 450 N normal load is applied in wet conditions the tribological behaviour is very different. The total wear remains negative and gradually decreases. Negative wear in Fig. 5a for both wet and dry conditions and negative wear in Fig. 5b only for relative humidity of 15% indicate material build-up on the coating surface; this is caused by the formation of a thick oxide layer under high surface temperature conditions (e.g. due to high load and sliding speed) and subsequent wear debris transfer from the pin to the disk. The oxide developed on the surface may be partially removed or retained as freely-moving particles between the contacting materials, acting as three-body abrasives. If the oxide layer is well adherent to the metal substrate, it can continue to thicken and reduce the metal/ceramic contact, providing protection against wear damage [11].

The positive wear during the second part of the tests is due to fragmentation of the tribolayer. When a 650 N normal load is applied at the humidity of 95% the wear reverses its trend for a shorter sliding distance than in dry conditions. When the relative humidity is increased the surface temperatures are reduced by the water adsorption on ceramic coatings. In wet conditions the tribolayer is thinner than in dry conditions, providing less effective wear protection. As the test proceeds, the water desorption on the Cr_2O_3 coating and the partial removal of the oxide layer determine the progressive increase of the total wear. When a 450 N normal load is applied in wet conditions (Fig. 5b) the water adsorption on the ceramic coating and the lower contact pressure prevent the surface temperature from increasing. It is well known that oxide surfaces adsorb water either dissociatively or molecularly. If water is dissociatively adsorbed many strongly bound surface hydroxyl groups are formed on the surface. The water desorption on Cr_2O_3 occurs above 500 °C and leads to a surface structure, which cannot be recovered by rehydroxylation of the surface [28,29]. In this case the surface temperature is widely lower than 500 °C and the total wear remains negative for the duration of the test. Some authors also suggest that the reduction of the oxidation rate is due to the formation of iron hydroxide and ferri-oxide-hydrate [13,14]. These oxides can act as protective layers preventing metal/ceramic interaction.

Fig. 6a shows the wear scar profiles of the disks under different normal load and relative humidity conditions. It can be seen that the depth of the wear track increases in the following order $450\text{N_RU95\%} < 450\text{N_RU15\%} < 650\text{N_RU95\%} < 650\text{N_RU15\%}$. When a normal load of 450 N is applied in wet conditions, no wear

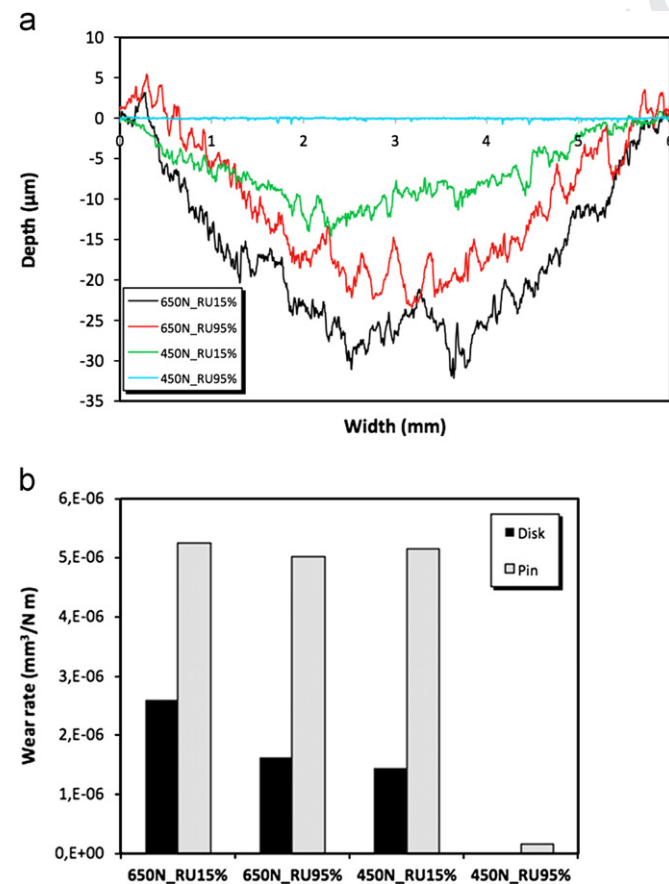


Fig. 6. (a) Wear scar profiles of disks under different normal load and relative humidity conditions and (b) Wear rate of pins and disks under the same different conditions (For interpretation of the references to color in this figure, the reader is referred to the web version of this article).

damage is found and the wear scar profile (blue line in Fig. 6a) is comparable with the roughness of the ceramic coating. In contrast, when the same load is applied in dry conditions, metallic film transfer occurs on the Cr_2O_3 coating due to localised melting of the oxide interlayers. Correspondingly, isolated peaks are observed inside the wear track (green line in Fig. 6a). When a 650 N normal load is applied in dry and wet conditions, a greater quantity of peaks inside the wear tracks is observed (red and black lines in Fig. 6a). Moreover, some other peaks can be seen at the edges of the wear tracks. The sliding motion between metal and ceramic is accompanied by the formation of wear debris. Some of these particles are thrown out from the contact area and accumulated along the sides of the sliding tracks.

Fig. 6b depicts the wear rate of pins and disks under the same different normal load and relative humidity conditions. In any case, the pin undergoes a significant loss of material. Except for a 450 N normal load applied in wet conditions, the wear rate is approximately $5 \times 10^{-6} \text{ mm}^3/(\text{N m})$. When a 450 N load is applied in wet conditions, the wear rate is one order of magnitude lower than those for the other pins. Many studies concerning the tribological behaviour of high carbon steels in dry sliding suggested that if the wear rate is greater than $1 \times 10^{-8} \text{ mm}^3/(\text{N m})$, the wear can be considered as severe wear. Moreover, they found the greater wear rate corresponds to the higher friction temperature [30–33]. The wear rate of the disks decreases in the following order

$650\text{N_RU15\%} > 650\text{N_RU95\%} > 450\text{N_RU15\%}$. However, when a 450 N normal load is applied in dry conditions, the wear rate is comparable with the value obtained when a 650 N normal load is applied in dry conditions. No wear rate is indicated for the disk when a 450 N normal load is applied in wet conditions, because the wear damage is three orders of magnitude lower than all the others.

The SEM micrographs of the coating worn surface, for a 650 N normal load applied in dry conditions, are shown in Fig. 7a–c. The material transfer from the metallic pin onto the ceramic surface can be seen (Fig. 7a). In particular, the wear scar with metallic film deposition could be divided into two zones. The first one is covered by a smooth iron oxide layer (Fig. 7b). It is in good agreement with previous studies, which show that, if the thermal conductivity of a material is not sufficiently high, the surface temperature can exceed the melting temperature. Consequently, the melting of local areas on the worn surfaces and the subsurface layers can be observed. Some works show that localised melting occurs not only at higher normal loads and sliding speeds, but even at sliding speeds as low as 1 m/s [20,33,34]. Metallic film is firmly attached to the Cr_2O_3 coating, because of the strong adhesion between the sliding surfaces: it is plastically deformed and oriented in the direction of the sliding motion. Scratches and local plastic deformations are indicated in Fig. 7b. This adhesive metal transfer justifies the peculiar pattern of the ceramic wear scar profile observed in Fig. 6a. In the second zone, many pits are uniformly distributed over the wear track (Fig. 7c): wear debris in the form of flakes is also generated. During sliding in dry conditions, microcracks and dislocation networks can produce fine wear debris as observed in the worn surface. Some wear particles are entrapped in the contact interface and subjected to continued fracture, deformation or chemical reaction, producing microsized powders. It can be demonstrated that at higher loads, wear debris cannot be taken away and the amount of wear particles deposited on the worn surface increases with the applied normal load. Moreover, smooth oxide layers are bigger and the scratches are deeper in higher loading conditions [23,35].

Fig. 8 shows the SEM micrograph of the worn coating surface and results from corresponding EDS analyses, when a 650 N normal load is applied in dry conditions. EDS analysis on the

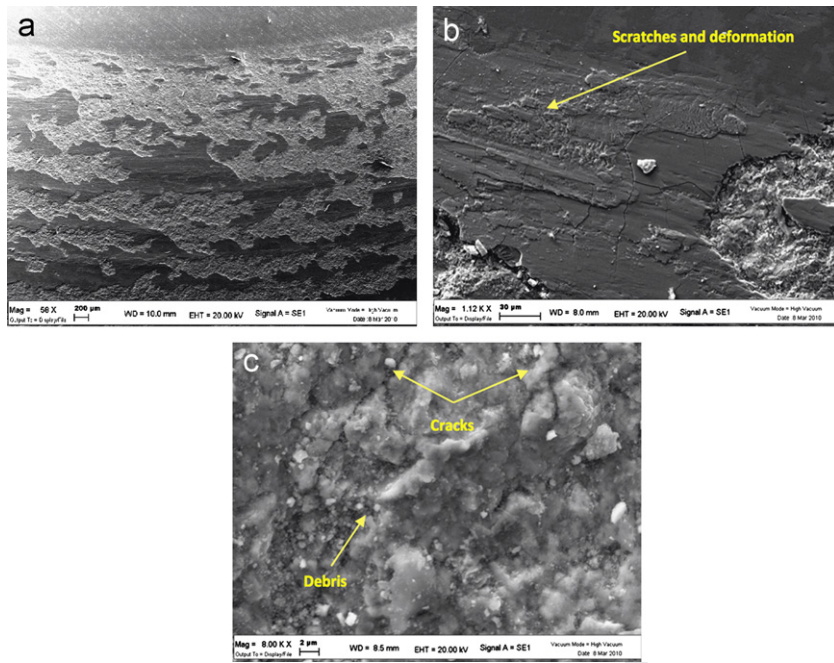


Fig. 7. SEM micrographs of Cr_2O_3 worn surface for a 650 N normal load applied in dry conditions: (a) overview of wear scar, (b) detail of metallic film transfer and (c) details of cracks and wear debris.

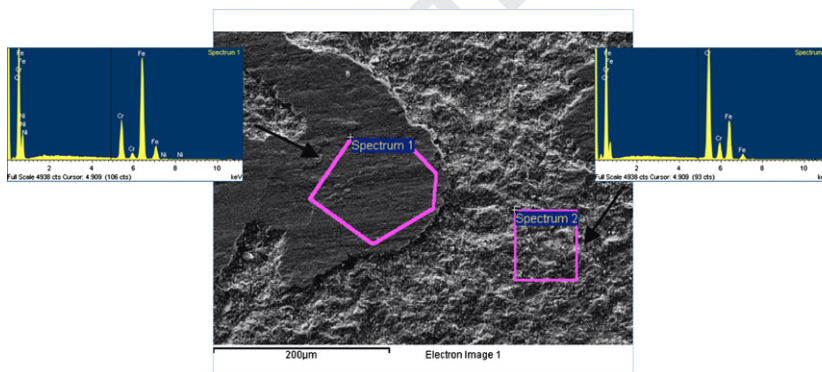


Fig. 8. Results from SEM micrograph and EDS analysis of Cr_2O_3 worn surface, when a 650 N normal load is applied in dry conditions.

metallic film indicates the presence of a great amount of iron and traces of other alloying elements such as chromium and nickel, transferred onto the ceramic coating. In contrast, EDS analysis of the original ceramic surface indicates the presence of a great amount of chromium and traces of iron as wear particles. A subsequent X-ray diffractometry examination enabled the type of film to be distinguished (Fig. 9). It is a Fe_2O_3 compound, which generally forms when the contact temperature rises over about 200°C . A comparison between Fig. 9 and Fig. 2 shows that the Cr_2O_3 coating does not change its crystal structure after the wear test.

When a 650 N normal load is applied in wet conditions and a 450 N normal load is applied in dry conditions (Fig. 10), the morphology of the coating of the worn surfaces and the wear mechanisms are similar to the previous case. The SEM micrograph in Fig. 10a depicts an overview of the wear scar. The amount of smooth oxide layers can be compared to the metal transfer observed in Fig. 7a, but the scratches are shallow. Fig. 10b shows the details of fracture on the original ceramic surface. In agreement with the microstructure of the coating, it can be seen that

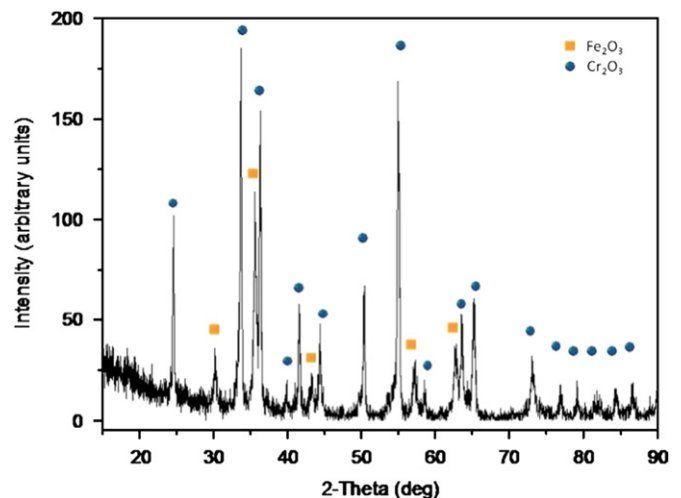


Fig. 9. XRD pattern of Cr_2O_3 worn surface for a 650 N normal load applied in dry conditions.

microfractures develop along the columnar grains in a perpendicular direction to the surface and along the splat boundaries since their strength is usually not high enough. At higher magnification, pits are also visible (Fig. 10c).

When a 450 N normal load is applied in wet conditions, no wear damage is observed on the ceramic coating (Fig. 11a). The surface appears smoother without evidence of significant wear and the pores remain open in the flattened surface (Fig. 11b).

The SEM micrographs of the worn surface of a pin for a 650 N normal load applied in dry conditions and a 450 N normal load

applied in wet conditions are shown in Fig. 12a and b, respectively. In the first case (Fig. 12a), the surface is very rough and plastically deformed with the ploughing appearance typical of adhesive wear. A thick film of iron oxide covers the worn surface with a mainly dark grey colour as revealed by optical microscopic observations (Fig. 13). The metallic film is discontinuous, indicating that the wear mechanism involves both the removal and re-formation of the oxide film and wears the free metallic surface. Many studies suggest that, in the mild-oxidational wear regime, oxidation is caused by frictional heat. The oxide film grows until it reaches a

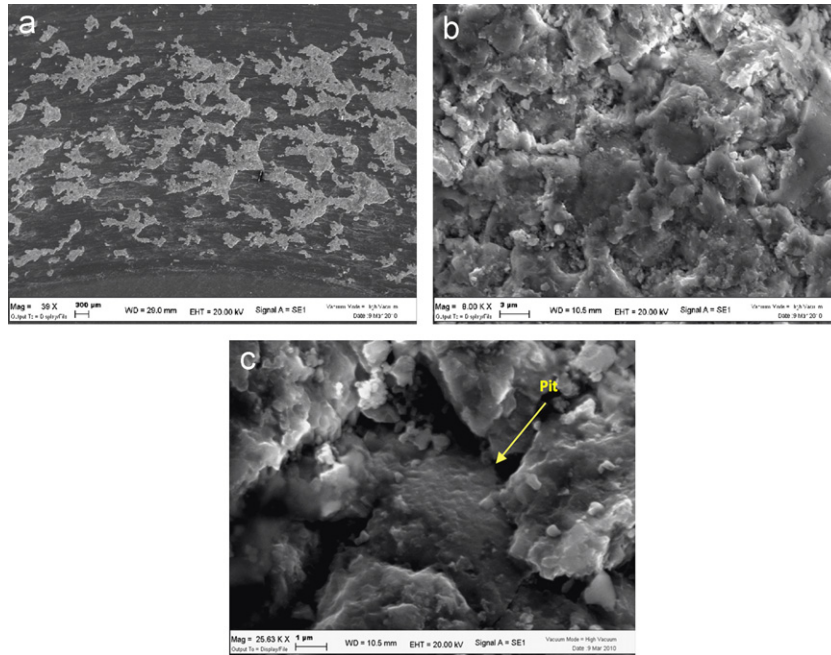


Fig. 10. SEM micrographs of Cr_2O_3 worn surface, when a 450 N normal load applied in dry conditions: (a) overview of wear scar, (b) details of cracks and wear debris and (c) detail of a pit.

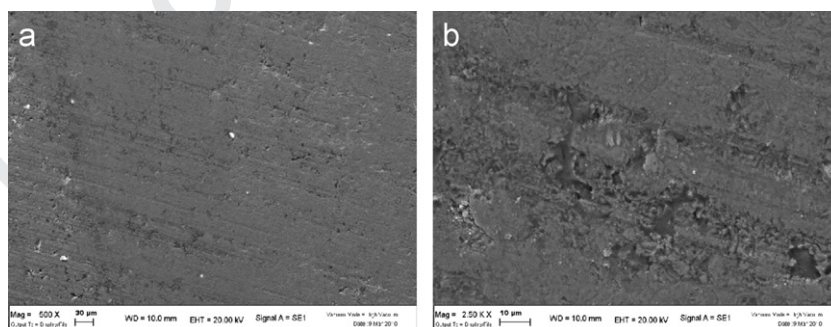


Fig. 11. SEM micrographs of Cr_2O_3 worn surface for a 450 N normal load applied in wet conditions: (a) overview of wear scar and (b) detail of open porosity.

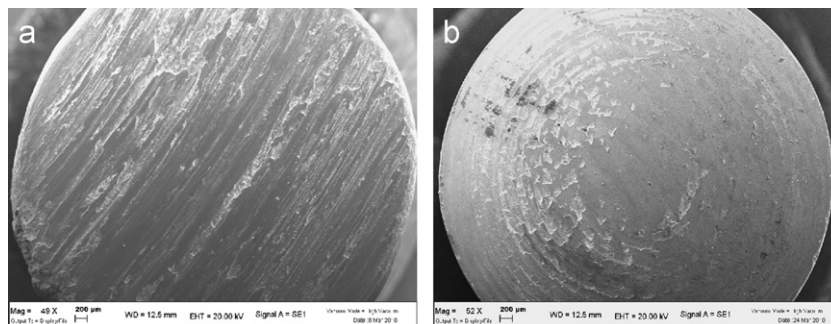


Fig. 12. SEM micrographs of worn surface of pins: (a) for a 650 N normal load applied in dry conditions and (b) when a 450 N normal load is applied in wet conditions.

critical thickness (about 10 μm for steel), then it spalls off as wear debris. For high normal loads and sliding speeds a transition to severe-oxidational wear can occur. This is associated with the localised melting of the oxide layer to a viscous liquid that can flow under the sliding action. This time, the melt-dominated wear replaces adhesion and delamination-dominated mechanisms [10,11,31–33]. When a 650 N normal load is applied in wet conditions and a 450 N normal load is applied in dry conditions, the morphology of the worn surfaces of the pin and the wear mechanisms are similar to the previous case. When a 450 N normal load is applied in wet conditions, no significant wear damage is observed (Fig. 12b). Only a small amount of metallic oxide appears on the worn surface of the pin. Moreover, the working marks are still visible.

For a 650 N normal load applied in dry conditions, optical microscope observations of the cross-sections of the pin can provide information about the dynamic changes in worn surface layers (Fig. 13). The sliding wear between the metal and ceramic surfaces results in a laminated structure. In particular, it consists of an iron oxide layer about 10 μm -thick (A); a layer of a very fine structure without a defined position and orientation (B); a fine structure with a clearly defined position and orientation (C); a plastically deformed layer (D) and the unaffected structure (E). It is well known that, for a given material, the characteristic structural layers appear depending on test conditions. In general, the thickness of the plastically deformed layer is related to the properties of the material itself. Structures with low plasticity and low thermal conductivity (e.g. martensite) are difficult to deform. This results in a higher surface temperature and a thinner plastically deformed layer. In contrast, structures with good plasticity and high thermal conductivity (e.g. pearlite) are easier to deform and less heat accumulates on the surface. Accordingly, a thicker plastically deformed layer can form. The morphology of the material build-up, accumulated at the edge of the worn surface of the pin is

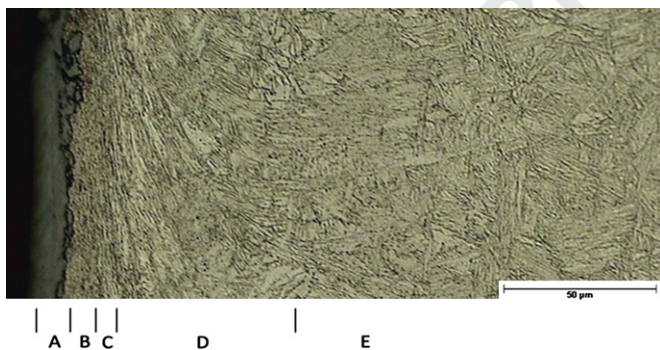


Fig. 13. Optical micrograph of worn surface of a pin, when a 650 N normal load is applied in dry conditions.

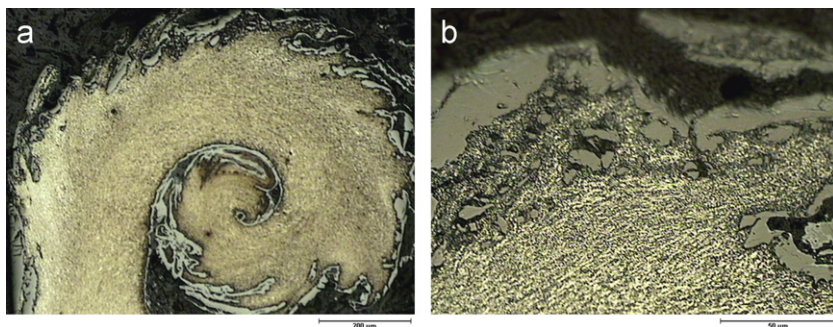


Fig. 14. Optical micrographs of worn surface of a pin, when a 650 N normal load is applied in dry conditions: (a) detail and (b) microstructure of material build-up at edge of sliding surface.

observed in Fig. 14a. It is plastically deformed due to the sliding motion and the highest surface temperature. It also consists of a very fine sorbitic microstructure with a great amount of uniformly distributed carbides (Fig. 14b). Optical microscope examinations of the cross-sections of the pins, for a 450 N normal load applied in wet conditions, show the same microstructure found before the wear test (Fig. 15). No evidence of a laminated structure or the material build-up, accumulated at the edge of the worn surface of the pin, is observed.

Fig. 16a shows the microhardness profiles of the worn surfaces of the pin, when a 650 N normal load is applied in different conditions. It can be seen that there is a very narrow region just below the worn surface with high microhardness. Both curves rapidly decrease and reach values comparable to the microhardness of the base un-cemented material. During sliding wear, friction energy is used to produce plastic deformation and heat. Strain gradient and temperature gradient in worn surface layers affect the hardness distribution. Many internal factors affect the hardness of the worn surface layers of the steel, such as strain hardening, recovery and recrystallisation, precipitation hardening, thermal martensitic transformation, tempering and so on. Therefore, the hardness profiles measured after the wear tests reflect the competition between the factors that cause hardening and those that cause softening. It can also be demonstrated that an originally softer microstructure, which has a higher value of the work hardening coefficient (e.g. pearlite), is likely to show hardening. An originally harder microstructure, which has a lower value of the work hardening coefficient (e.g. martensite), is likely to show softening. This is in accordance with the rapid decrease in the microhardness profile observed in Fig. 16a. The wear volume is also related to the hardening and softening behaviour resulting from dynamic changes in the worn surface layers. Generally, a smaller softening response corresponds to better wear resistance [31–33]. When a 450 N normal load is applied in dry conditions the softening trend of surface layers is the same as the previous cases (Fig. 16b). For a 450 N normal load applied in wet conditions, the microhardness profile is typical of steels subjected to hardening surface treatment. There is no evidence of strain hardening or softening due to the sliding wear.

4. Conclusions

Based on the results obtained regarding friction and wear behaviour of a carbon steel in sliding contact with a Cr_2O_3 plasma-sprayed ceramic coating, the following conclusions can be drawn:

- In dry and wet conditions, wear rates of the ceramic coating decrease with normal load. In dry conditions, wear rates of the pins are independent of the normal loads applied. For a lower

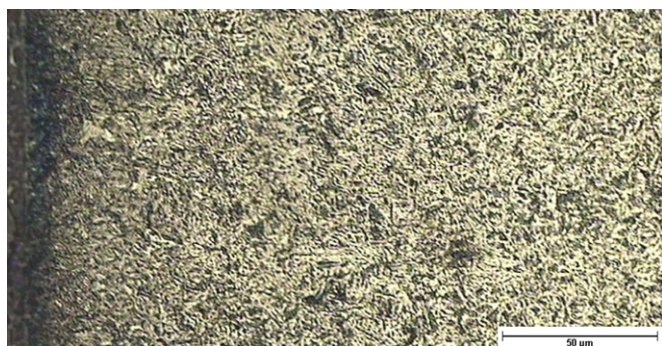


Fig. 15. Optical micrograph of a worn pin surface, when a 450 N normal load is applied in wet conditions.

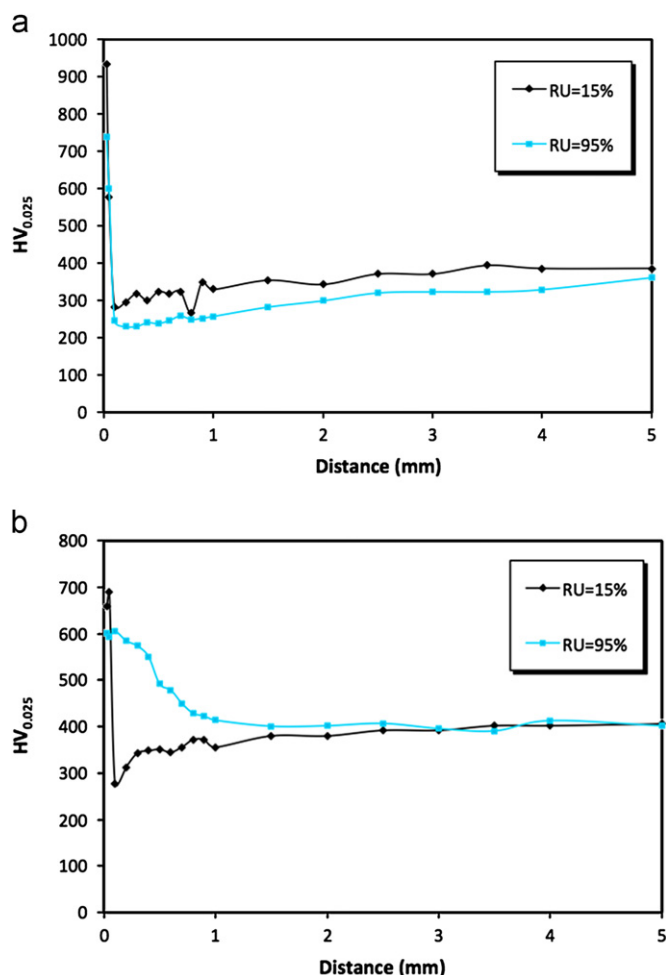


Fig. 16. Microhardness profiles of worn surfaces of pins when: (a) 650 N and (b) 450 N normal loads are applied in different humidity conditions.

normal load applied in wet conditions, the wear rate of the pins is reduced by about six orders of magnitude.

- For all the normal loads applied in dry conditions, metal/ceramic sliding contact produces a metallic film transfer onto the ceramic surface. Metallic film consists of a Fe_2O_3 compound usually formed at temperatures over about 200°C . The presence of this oxide suggests a progressive increase in the contact temperatures as the wear tests proceed. The observations of the worn surfaces of the pins indicate that the principal wear mechanism involved is mild-oxidational wear, with ploughing and a plastic deformation appearance. The dynamic changes in the surface

layers of the material also result in a laminated structure. The subsequent transition to severe-oxidational wear is associated with the localised melting of the oxide layer and its spreading on the ceramic surface. Considering the ceramic coating, the observations of Cr_2O_3 worn surfaces show that it undergoes microfracture along the splat and columnar grains boundaries.

- In wet conditions, the normal load applied influences the tribological behaviour of the metal/ceramic sliding couplings. For the highest normal load the wear mechanisms are the same as those in dry conditions. For the lower normal load the reduction of the surface temperatures and, consequently, of the oxidation rate, is due to the water adsorption on the worn surfaces. The moisture adsorbed can act as a protective layer preventing metal/ceramic interaction.

Acknowledgements

The authors would like to thank Zocca Officine Meccaniche (Funò, BO) for the thermally sprayed coating manufacturing, and Engineer Marco Vitali for his contribution to the experimental activity.

References

- [1] H.A. Bolton, J.M. Larson, *Valvetrain System Design and Materials*, ASM International, Materials Park, OH, 2002.
- [2] C.T. Sims, N.S. Stoloff, W.C. Hagel, *Superalloys II: High Temperature Materials for Aerospace and Industrial Power*, Wiley-Interscience, New York, 1987.
- [3] M.J. Donachie, S.J. Donachie, *Superalloys—a Technical Guide*, ASM International, Materials Park, OH, 2002.
- [4] F.H. Stott, D.S. Lin, G.C. Wood, *Glazes* produced on nickel-base alloys during high temperature wear, *Nature* 242 (1973) 75–77.
- [5] F.H. Stott, D.S. Lin, G.C. Wood, The structure and mechanism of formation of the 'glaze' oxide layers produced on nickel-based alloys during wear at high temperatures, *Corrosion Science* 13 (6) (1973) 449–469.
- [6] P.J. Blau, T.M. Brummett, B.A. Pint, Effects of prior surface damage on high-temperature oxidation of Fe-, Ni, and Co-based alloys, *Wear* 267 (2009) 380–386.
- [7] F.H. Stott, G.C. Wood, The influence of oxides on the friction and wear of alloys, *Tribology International* 11 (4) (1978) 211–218.
- [8] T.F.J. Quinn, Review of oxidational wear. Part I: The origins of oxidational wear, *Tribology International* 16 (5) (1983) 257–271.
- [9] S.C. Lim, M.F. Ashby, *Overview no.55 Wear-mechanism maps* 35 (1) (1987) 1–24. *Acta Metallurgica* 35 (1) (1987) 1–24.
- [10] F.H. Stott, High-temperature sliding wear of metals, *Tribology International* 35 (8) (2002) 489–495.
- [11] F.H. Stott, The role of oxidation in the wear of alloys, *Tribology International* 31 (1–3) (1998) 61–71.
- [12] P.J. Blau, Elevated-temperature tribology of metallic materials, *Tribology International* 43 (2010) 1203–1208.
- [13] W.Y.H. Liew, Effect of relative humidity on the lubricated wear of metals, *Wear* 260 (7–8) (2006) 720–727.
- [14] P. De Baets, G. Kalacska, K. Strijckmans, F. Van De Velde, A.P. Van Peteghem, Experimental study by means of thin layer activation of the humidity influence on the fretting wear of steel surfaces, *Wear* 216 (2) (1998) 131–137.
- [15] H. Goto, D.H. Buckley, The influence of water vapour in air on the friction behaviour of pure metals during fretting, *Tribology International* 18 (4) (1985) 237–245.
- [16] G. Bregliozzi, S.I.-U. Ahmed, A. Di Schino, J.M. Kenny, H. Haefke, Friction and wear behaviour of austenitic stainless steel: influence of atmospheric humidity, load range, and grain size, *Tribology Letters* 17 (2004) 697–704.
- [17] E. Tsuji, A. Ando, Effects of air and temperature on speed dependency of sliding wear of steel, in: Proceedings of JSLE ASLE International Lubrication Conference, Tokyo, 1975 pp. 101–109.
- [18] S. Asanabe, Applications of ceramics for tribological components, *Tribology International* 20 (1987) 355–364.
- [19] V. Aronov, T. Mesyef, Wear in ceramic/ceramic and ceramic/metal reciprocating sliding contact. Part1, in: Proceedings of ASME/ASLE Joint Tribology Conference, Atlanta, 1985 pp. 16–21.
- [20] G.W. Stachowiak, G.B. Stachowiak, A.W. Batchelor, Metallic film transfer during metal–ceramic unlubricated sliding, *Wear* 132 (2) (1989) 361–381.
- [21] B. Wang, Z.R. Shui, A.V. Levy, Sliding wear of thermally sprayed chromia coatings, *Wear* 138 (1990) 93–110.
- [22] A. Tronche, P. Fauchais, Frictional behaviour against steel of aluminium substrates plasma-sprayed with hard coatings, *Materials Science and Engineering A* 102 (1988) 1–12.

- [23] H. Cetinel, E. Celik, M.I. Kusoglu, Tribological behaviour of Cr₂O₃ coatings as bearing materials, *Journal of Materials Processing Technology* 196 (1–3) (2008) 259–265.
- [24] J.E. Fernandez, Y. Wang, R. Tucho, M.A. Martin-Luengo, R. Gancedo, A. Rincón, Friction and wear behaviour of plasma-sprayed Cr₂O₃ coatings against steel in a wide range of sliding velocities and normal loads, *Tribology International* 29 (4) (1996) 333–343.
- [25] C.B. Ponton, R.D. Rawlings, Vickers indentation fracture toughness test—Part 1: review of literature and formulation of standardised indentation toughness equation 5 (1989) 865–872 *Materials Science and Technology* 5 (1989) 865–872.
- [26] C.B. Ponton, R.D. Rawlings, Vickers indentation fracture toughness test—Part 2: application and critical evaluation of standardised indentation toughness equations 5 (1989) 961–976 *Materials Science and Technology* 5 (1989) 961–976.
- [27] G. Bolelli, V. Cannillo, L. Lusvarghi, T. Manfredini, Wear behaviour of thermally sprayed ceramic oxide coatings, *Wear* 261 (2006) 1298–1315.
- [28] S. Kittaka, K. Morishige, J. Nishiyama, T. Morimoto, The effect of surface hydroxyls of Cr₂O₃ on the adsorption of N₂, Ar, Kr, and H₂O in connection with the two-dimensional condensation, *Journal of Colloid and Interface Science* 91 (1) (1983) 117–124.
- [29] M. Harju, T. Mäntylä, K. Vähä-Heikkilä, V. Lehto, Water adsorption on plasma sprayed transition metal oxides, *Applied Surface Science* 249 (1–4) (2005) 115–126.
- [30] E. Takeuchi, Friction and wear of machine parts—surface heat treatments for increase wear resistance, *Machine Tools* 23 (5) (1979) 68–74.
- [31] Y. Wang, T. Lei, J. Liu, Tribo-metallographic behaviour of high carbon steels in dry sliding—I. Wear mechanisms and their transition, *Wear* 231 (1999) 1–11.
- [32] Y. Wang, T. Lei, J. Liu, Tribo-metallographic behaviour of high carbon steels in dry sliding—II. Microstructure and wear, *Wear* 231 (1999) 12–19.
- [33] Y. Wang, T. Lei, J. Liu, Tribo-metallographic behaviour of high carbon steels in dry sliding—III. Dynamic microstructural changes and wear, *Wear* 231 (1999) 20–37.
- [34] X.D. Li, Y. Wang, J.J. Liu, A study on dry friction of eutectoid steel, *Wear* 150 (1991) 59–65.
- [35] H.S. Ahn, O.K. Kwon, Wear behaviour of plasma-sprayed partially stabilized zirconia on a steel substrate, *Wear* 225–229 (1999) 814–824.

17
18
19
20
21
22
23
24
25
26
27
28
29
30
31

UNCORRECTED PROOF